

1
2 MR. MARC B. BIREN (Orcid ID : 0000-0002-3410-1892)

3 DR. CHRISTIAN KOEBERL (Orcid ID : 0000-0001-5155-7405)

4
5
6 Article type : Article

7
8
9 (U-Th)/He zircon dating of Chesapeake Bay distal impact
10 ejecta from ODP site 1073

11
12 M.B. Biren^a, J-A. Wartho^{a,b}, M.C. van Soest^a, K.V. Hodges^a, H. Cathey^{c,d}, B.P. Glass^e, C.
13 Koerberl^f, J.W. Horton Jr.^g, and W. Hale^h

14 ^aGroup 18 Laboratories, School of Earth and Space Exploration, Arizona State University,
15 Tempe, AZ 85287, USA. Contact: marc.biren@asu.edu.

16 ^bGEOMAR Helmholtz Centre for Ocean Research Kiel, D-24148 Kiel, Germany

17 ^cLeRoy Eyring Center for Solid State Science, Arizona State University, Tempe, AZ 84287,
18 USA

19 ^dCentral Analytical Research Facility, Queensland University of Technology, Brisbane, QLD
20 4000, Australia

21 ^eDepartment of Geological Sciences, University of Delaware, Newark, DE 19716, USA.

22 ^fDepartment of Lithospheric Research, University of Vienna, A-1090 Vienna, Austria, and
23 Natural History Museum, Burgring 7, A-1010 Vienna, Austria.

24 ^gU.S. Geological Survey, 926A National Center, Reston, VA 20192, USA.

25 ^hIODP Core Repository, Bremen D-28359, Germany.

26
27 **Abstract**

This is the author manuscript accepted for publication and has undergone full peer review but has not been through the copyediting, typesetting, pagination and proofreading process, which may lead to differences between this version and the [Version of Record](#). Please cite this article as [doi: 10.1111/MAPS.13316-3135](https://doi.org/10.1111/MAPS.13316-3135)

This article is protected by copyright. All rights reserved

28 Single crystal (U-Th)/He dating has been undertaken on 21 detrital zircon grains
29 extracted from a core sample from Ocean Drilling Project (ODP) site 1073, which is located
30 ~390 km northeast of the center of the Chesapeake Bay impact structure. Optical and electron
31 imaging in combination with energy dispersive X-ray microanalysis (EDS) of zircon grains from
32 this late Eocene sediment show clear evidence of shock metamorphism in some zircon grains,
33 which suggests that these shocked zircon crystals are distal ejecta from the formation of the ~40
34 km diameter Chesapeake Bay impact structure. (U-Th/He) dates for zircon crystals from this
35 sediment range from 33.49 ± 0.94 to 305.1 ± 8.6 Ma (2σ), implying crystal-to-crystal variability
36 in the degree of impact-related resetting of (U-Th)/He systematics and a range of different
37 possible sources. The two youngest zircon grains yield an inverse-variance weighted mean (U-
38 Th)/He age of 33.99 ± 0.71 Ma (2σ uncertainties $n = 2$; Mean Square Weighted Deviation
39 (MSWD) = 2.6; Probability (P) = 11 %), which is interpreted to be the (U-Th)/He age of
40 formation of the Chesapeake Bay impact structure. This age is in agreement with K/Ar,
41 $^{40}\text{Ar}/^{39}\text{Ar}$, and fission track dates for tektites from the North American strewn field, which have
42 been interpreted as associated with the Chesapeake Bay impact event.

43

44 **1. Introduction**

45 The largest well-preserved impact structure in the United States of America lies hidden
46 beneath part of Chesapeake Bay (Fig. 1), near the southwestern tip of the Delmarva Peninsula in
47 Virginia (Horton et al., 2009). Seismic profiles and gravity data were used to locate the
48 Chesapeake Bay structure, and its impact origin was later confirmed by the presence of shocked
49 quartz and feldspar grains observed within various drill core samples (e.g., Poag et al., 1992,
50 1994; Koeberl et al., 1996; Harris et al., 2004; Horton and Izett, 2005; Horton et al., 2009). The
51 impact structure represents a complex crater that is roughly centered on the town of Cape
52 Charles and exhibits an 85 km-diameter outer damage zone of collapsed and mobilized
53 sediments and a 40 km-diameter central crater (Fig. 1; Collins and Wünnemann, 2005; Horton
54 and Izett, 2005). The Chesapeake Bay impact structure is thought to be the source crater for the
55 North American tektite (NAT) strewn field (Fig. 2; e.g., Horton and Izett, 2005; Deutsch and
56 Koeberl, 2006; Koeberl, 2009), including tektites and ejecta material found preserved both
57 onshore and offshore.

58 Previous attempts to determine the age of impact structures, such as the Chesapeake Bay
59 crater, have mainly focused on the use of $^{40}\text{Ar}/^{39}\text{Ar}$ or U/Pb geochronometers (e.g., Jourdan et
60 al., 2012 and references therein). Recently, (U-Th)/He thermochronology of apatite, titanite, and
61 zircon has proven to be another valuable isotopic system for this purpose (e.g., Ukstins Peate et
62 al., 2010; van Soest et al., 2011; Wartho et al., 2012; Young et al., 2013a, b; Biren et al. 2014;
63 2016; Wielicki et al., 2014). In order to augment previous attempts to date the Chesapeake Bay
64 event using a variety of isotopic and fission-track chronometers, we have used the (U-Th)/He
65 method to date 21 individual zircon grains in an unconsolidated sediment from ODP site 1073
66 hole A, located ~390 km north-east of the Chesapeake Bay impact structure (Fig. 2). This section
67 of core contains ejecta products presumably related to the Chesapeake Bay structure, and thus
68 might be expected to offer an opportunity to determine (U-Th)/He closure dates for zircon
69 crystals that may have had their helium isotopic systematics disturbed or reset at the time of the
70 impact event.

71 Zircon crystals ejected from the Chesapeake Bay impact crater and distally deposited on
72 the sea floor would have the advantage of being cooled very rapidly, in contrast to zircon grains
73 sourced from proximal impactites within a hot and slowly cooling crater. This is especially
74 important considering the relatively low He closure temperature of zircon (~200 °C; Reiners et
75 al., 2004). $^{40}\text{Ar}/^{39}\text{Ar}$ or U/Pb geochronometers have recently been used to examine different
76 settings (slow crater cooling and hydrothermal resetting/alteration vs. rapid ejecta cooling) in
77 relation to hydrothermally-reset vs. impact-formation ages, respectively (Schmieder et al., 2018;
78 Kenny et al., 2019).

79

802 1.1 Geological context

81 The Chesapeake Bay impact structure was formed on the continental margin of Virginia
82 in a shallow-marine sequence of 200-500 m of seawater, 600-1000 m of Cretaceous to Eocene
83 unconsolidated sediments, and underlying Proterozoic to Paleozoic crystalline rocks (Kamo et
84 al., 2002; Collins and Wünnemann, 2005; Horton and Izett, 2005). The Chesapeake Bay impact
85 structure is also associated with distal ejecta found onshore in Georgia (the tektite deposits are
86 termed georgirites), Texas (bediasites), Massachusetts (Martha's Vineyard), and Barbados, and
87 offshore in the Caribbean Sea (Deep Sea Drilling Project (DSDP) site 149), the Gulf of Mexico

88 (DSDP site 94), and the continental shelf of the NW Atlantic (DSDP site 612; ODP sites 903
89 and 1073; Fig. 2; e.g., Glass and Liu, 2001; Glass, 2002; Simonson and Glass, 2004).

90

91 **1.2 Previous age determinations for the Chesapeake Bay impact structure**

92 The age of the Chesapeake Bay impact structure has been inferred indirectly from K/Ar,
93 fission track, and $^{40}\text{Ar}/^{39}\text{Ar}$ dates of NAT ranging from 32.5 ± 2.0 to 35.9 ± 4.8 Ma (2σ ; Table 1;
94 e.g., Fernandes et al. 2019). In addition, TIMS U-Pb dating of 24 intensely shocked zircon
95 crystals from the NA microtektite layer from DSDP/ODP sites 612, 903 and 904 and Bath Cliff
96 in Barbados produced upper and lower intercept U-Pb Concordia ages of 400 ± 32 Ma and ~ 35.4
97 Ma, respectively (Kamo et al., 2002).

98

99 **1.3 Sample Description**

100 A ~ 30 cm³ core sample of upper Eocene unconsolidated glauconite-bearing sediment
101 (Fig. 3) was obtained from ODP site 1073, hole A, core 72X (depth range of core 72X = 654.1 -
102 663.6 meters below sea floor), section 4, interval 83-94 cm, obtained during ODP Leg 174A
103 expedition (Austin et al., 1998), from the International Ocean Drilling Project (IODP) Bremen
104 Core Repository in Germany. The upper Eocene interval of the 1073 drill hole A mainly consists
105 of clay-rich nannofossil chalk and diatom-rich nannofossil clay that is strongly bioturbated
106 (Austin et al., 1998). Unmelted impact ejecta (> 125 μm) are confined to an interval between 61-
107 120 cm in core 72-4, with numerous white (opaque) grains of shock metamorphosed quartz and
108 K-feldspar with planar deformation features. Coesite and reidite are also present in this interval,
109 but no microtektites or clinopyroxene-bearing spherules have been identified (Liu et al., 2006).
110 Dark green glauconite clays, sand and pellets are present below, above, and throughout the ejecta
111 layer, but form an abundance maximum associated with the ejecta layer (Liu and Glass, 2001).

112

113 **2. Analytical Methods**

114 The unconsolidated sediment sample was disaggregated and cleaned with deionized
115 water in an ultrasonic bath and then wet-sieved. The heavy minerals were separated using
116 standard gravimetric and magnetic techniques. A Leica MZ16 binocular microscope was used to
117 select and accurately measure the dimensions of twenty-one zircon grains for dating using the
118 (U-Th)/He method (Table 2). Individual zircon crystals were photographed and measured on at

119 least 2 different crystal faces, and loaded into individual 0.7 mm OD x 1.0 mm long Nb tubes
120 prior to isotopic analysis

121 (U-Th)/He analyses were undertaken in the Group 18 Laboratories at Arizona State
122 University. An Australian Scientific Inc. *Alphachron Mk II* helium extraction and analytical
123 system was employed for the helium isotopic analyses. On this system, an infrared (980 nm)
124 diode laser is used to heat Nb-encapsulated samples *in vacuo*. Evolved gases were purified using
125 hot and cold SAES NP10 getters prior to spiking with ^3He for isotope dilution analysis using a
126 Balzers QMS 200 quadrupole mass spectrometer. Blank Nb tubes and crystals of Fish Canyon
127 zircon were also analyzed in order to establish system blanks and monitor system performance.
128 The average ^4He blank was 0.049 femtomole for all procedures. ^4He abundances for the
129 unknowns were between 200-30000 times the blank for the zircon analyses. The concentration of
130 the ^4He aliquot pipetted from the ^4He standard tanks is known to within 1.18% (1σ), which for
131 most analyses, contributes the largest uncertainty to this part of the analytical process.

132 After helium extraction and analysis, the encapsulated zircon crystals were removed from
133 the Alphachron vacuum system, spiked with a solution of ^{230}Th and ^{235}U in 50% HNO_3 , and
134 dissolved in separate solutions of HF, HNO_3 and HCl acids using Parr digestion vessels at
135 elevated temperatures. U and Th isotopic ratios were measured by isotope dilution on a Thermo
136 Scientific *iCapQ* inductively coupled plasma source mass spectrometer (ICP-MS). Additional
137 details of the (U-Th)/He analytical procedures can be found in van Soest et al. (2011). (U-Th)/He
138 dates were calculated iteratively from blank-corrected ^4He , ^{232}Th , and ^{238}U concentrations. Raw
139 calculated dates were corrected for α -ejection based on optical measurements of the crystals
140 prior to analysis, following the protocols recommended by Farley et al. (1996). All (U-Th)/He
141 dates and inverse-variance mean ages are quoted in Table 2 with 2σ uncertainties.

142 Eight undated and unpolished zircon grains and grain fragments were mounted on sticky
143 carbon tape and photographed using a Leica MZ16 binocular microscope using the same
144 procedures as the dated grains. The grains were then carbon coated and examined using
145 secondary electron (SE) and backscattered electron (BSE) imaging and energy dispersive X-ray
146 spectrometry (EDS) with a JEOL JXA-8530F electron microprobe located at the John M.
147 Cowley Center for High Resolution Electron Microscopy, ASU. Operating conditions were 10
148 kV accelerating voltage and a 250 pA beam current. A low beam current was required to
149 minimize charging effects during the imaging session, during which spot analyses by EDS were

150 performed under the same conditions using a silicon drift diode (SDD) detector to confirm the
151 elemental compositions of the observed minerals and decompression melt phases, using
152 acquisition times of 25 seconds. Reported compositions utilize a ZAF matrix correction with
153 oxygen calculated by stoichiometry, and measurements were calibrated using an instrument-
154 specific mineral standard database.

155 These grains and grain fragments were not dated with the (U-Th)/He method because
156 they were too small or broken, plus the carbon coating required for SE/BSE/EDS analysis would
157 have caused a carbon contamination problem during the measurement of helium in the
158 quadrupole mass spectrometer, which is a common issue for noble gas mass spectrometer
159 analyses. However, the optical, SE, BSE, and EDS characteristics of this sub-set of zircon grains
160 are considered to be representative of the dated population of 21 zircon grains.

161

162 **3. Results**

163 Optical photomicrographs of the eight youngest (U-Th)/He dated zircon grains reveals
164 the presence of: (1) clear euhedral zircon crystals (Figs. 4A-B, and 4F); (2) rounded slightly
165 cloudy translucent zircon grains (Figs. 4C-E, G); and (3) one milky white opaque rounded zircon
166 grain (Fig. 4H).

167 The presence of zircon is supported by EDS spectra from the eight undated unpolished
168 zircon grains/fragments that all show pronounced and resolvable X-ray peaks for Zr ($L\alpha$) and Si
169 ($K\alpha$) and by quantitative analyses of six grains which yield average weight (wt.) % values for
170 ZrO_2 of 69.2 ± 6.2 , SiO_2 of 28.6 ± 4.0 , and analytical totals of 97.9 ± 7.2 (2σ). Five of the eight
171 undated zircon grains/fragments are optically clear and euhedral, and these zircon
172 grains/fragments show no evidence of shock metamorphism in the SEM images (e.g., Figs. 5A.1-
173 5A.2 and B.1-B.2). Multiple linear features were observed in two undated zircon grains (Figs.
174 5C.2-C.3 and 5D.2-D.3) and are interpreted as planar deformation features. The optical
175 photomicrographs of these two zircon grains indicate cloudy regions (Fig. 5C.1) or a totally
176 translucent crystal (Fig. 5D.1) that correlate with the presence of planar deformation features,
177 observed in Figs. 5C.2-C.3 and 5D.2-D.3; such features are commonly observed in shock
178 metamorphosed zircon grains (e.g., Kamo et al., 1996; Wittmann et al., 2006; Schmieder et al.,
179 2015). One partially-rounded, opaque undated zircon grain (Fig. 5E.1) shows evidence of partial
180 decomposition, marked by the transformation of zircon to a micron-scale dendritic intergrowth

181 of baddeleyite (ZrO_2) and silica (SiO_2 , with an EDS analysis yielding a wt. % $\text{ZrO}_2/\text{SiO}_2$ ratio of
182 ~ 31 in the bright BSE regions of intergrowth, Figs. 5E.2-E.3). The baddeleyite + silica
183 assemblage mainly occurs along the rims of the zircon grain and along cracks.

184 As shown in Table 2 and Fig. 6A, the twenty-one individual (U-Th)/He zircon analyses
185 yield dates ranging from 33.49 ± 0.94 to 305.1 ± 8.6 Ma. Six of the 21 dates are younger than 70
186 Ma, and the three youngest dates are 36.7 ± 1.0 Ma, 34.6 ± 1.1 Ma, and 33.49 ± 0.94 Ma.

188 4. Discussion

189 Based on our microscope observations and information gleaned from the electron probe
190 analyses, we conclude that the zircon population sampled in ODP 1073 hole A shows various
191 degrees of shock deformation (Fig. 5). Evidence for shock metamorphism includes planar
192 deformation features (Figs. 5C.2-C.3 and 5D.2-D.3), granular texture, and decomposition from
193 zircon to a dendritic assemblage of baddeleyite and silica (Figs. 5E.2-E.3). The zircon to
194 baddeleyite + silica decomposition process is estimated to occur at extreme shock conditions
195 (Wittmann et al., 2006; 2009a, b; Schmieder et al., 2015; Timms et al., 2017). Shock
196 metamorphism commonly results in cloudy or opaque zircon grains, as observed by Bohor et al.
197 (1993) and Corfu et al. (2003), which is also observed in our optical photomicrographs (Figs.
198 5C.1, 5D.1 and 5E.1) and has been confirmed by SEM observations of these grains (Figs. 5C.2-
199 C.3, 5D.2-D.3 and 5E.2-E.3).

200 Our ODP sample is comprised a mix of unshocked, weakly-shocked, and intensely-
201 shocked (including granular texture) zircon grains. The shocked zircon grains likely represent
202 distal ejecta from the Chesapeake Bay impact structure due to the excavation/ejection process,
203 whereas the unshocked zircon crystals may be derived from (1) unshocked Chesapeake Bay
204 target rocks, (2) different sources unrelated to the impact, or (3) may represent contamination by
205 drilling mud (Andrews et al., 2016). ODP drilling procedures include the use of a sepiolite
206 drilling mud (Sea MudTM), which is produced by mixing material quarried from the Amargosa
207 Basin of Nevada with seawater to form a gel that is able to carry heavier particles out of the drill
208 hole. Drill cores can become contaminated with the drilling fluids due to the elevated water
209 pressure or via fracturing of the core during drilling. Intrusion of drilling mud is likely to be
210 greater in drill core sample lithologies that are unlithified, porous, or heavily fractured. U/Pb
211 TIMS and Secondary Ionization Mass Spectrometer (SIMS) dating of the Sea MudTM zircon

212 grains has yielded ages ranging from 1.89 to 2889 Ma (Andrews et al., 2016), but no (U-Th)/He
213 data exist for Sea Mud™ zircon grains and we thus cannot comparatively evaluate the possibility
214 of contamination in our drill core sample. However, the broad distribution of (U-Th)/He zircon
215 dates from this sample, with a distinctive, young cluster of dates (Fig. 6A), is similar to that
216 found in (U-Th)/He datasets for rocks collected from other impact structures (e.g., Ukstins Peate
217 et al., 2010; van Soest et al., 2011; Wartho et al., 2012; Young et al., 2013a, b; Biren et al., 2014;
218 2016), i.e., many dates distributed over a wide age range, with a number of comparatively tightly
219 clustered young dates (Fig. 6A). We interpret this distribution to be indicative of (1) variable
220 resetting of pre-impact zircon crystals in the target rocks (i.e., ~260-240 Ma Alleghanian
221 granites, pegmatites and metamorphic basement rocks; e.g., Gibson et al., 2009; Horton et al.,
222 2009); and (2) (U-Th)/He zircon cooling dates from different sources.

223 Two of the three youngest zircon crystals are optically distinctive from some of the other
224 (U-Th)/He dated zircon crystals (Fig. 4). Zircon 1073 Z13 (33.49 ± 0.94 Ma; Fig. 4H) has an
225 opaque milky white appearance, and is similar to the undated opaque zircon (Fig. 5E.1) that is
226 partially decomposed to baddeleyite and silica (Figs. 5E.2-E.3). Zircon 1073 Z21 (34.6 ± 1.1 Ma;
227 Fig. 4G) is translucent and partly cloudy and is similar in appearance to the undated cloudy and
228 translucent zircon grains/fragments that preserve planar deformation features (Figs. 5C.1-C.3 and
229 5D.1-D.3). However, Zircon crystal 1073 Z06 (36.7 ± 1.0 Ma; Fig. 4F) is clear and euhedral, and
230 is similar in appearance to (1) two of the older dated zircon grains (1073 Z04 and Z20; Figs. 4A-
231 B), and (2) two of the clear euhedral undated zircon grains (Figs. 5A.1-B.2) that preserve no
232 evidence of shock metamorphism (Figs. 5A.2 and 5B.2). Due to these observations, the zircon
233 1073 Z06 with a (U-Th)/He date of 36.7 ± 1.0 Ma, is excluded from our inverse variance
234 weighted mean age.

235 We suggest that the two youngest zircon grains may have been shock-metamorphosed
236 during the formation of the Chesapeake Bay impact event, ejected from the target area, and
237 deposited at ODP site 1073 hole A, which is presently ~390 km NE of the impact structure (Fig.
238 2). Thus, the inverse-variance weighted mean age of 33.99 ± 0.71 Ma ($n = 2$; MSWD = 2.6; $P =$
239 11 %; Fig. 6B) represents our best estimate of the (U-Th)/He age of the Chesapeake Bay impact
240 event.

241 Owing to the fast He diffusion parameters in zircon (Reiners et al., 2004) it is
242 advantageous to undertake (U-Th)/He studies on ejected heavy minerals found within tektite and

243 microtektite layers in distal marine deposits. These shock-metamorphosed distal zircon grains
244 would have undergone virtually instantaneous cooling via interaction with the air and seawater,
245 thereby yielding a reliable impact formation age. In contrast, geochronological analyses of
246 proximal and crater-filling impactite samples may suffer from the effects of prolonged post-
247 impact cooling and/or hydrothermal resetting/alteration, thus potentially yielding ages that are
248 younger than the impact formation event (e.g., Schmieder et al., 2018; Kenny et al., 2019).
249 $^{40}\text{Ar}/^{39}\text{Ar}$ studies indicate that medium sized (~23 km diameter) impact craters can host relatively
250 long-lived hydrothermal systems (> 1 Ma; Schmieder and Jourdan, 2013).

251 Our inverse variance-weighted mean (U-Th)/He age of 33.99 ± 0.71 Ma for Chesapeake
252 Bay is in agreement or slightly younger than previous ages obtained from analyses of NA tektites
253 by fission track, K/Ar, and $^{40}\text{Ar}/^{39}\text{Ar}$ dating methods (Fig. 7; Reynolds, 1960; Zähringer, 1963;
254 Fleischer and Price, 1964; Gentner et al. 1969; Garlick et al., 1971; Storzer and Wagner, 1971;
255 Glass et al., 1973; Bottomley et al., 1979; Storzer and Wagner, 1977; Bottomley, 1982; Glass et
256 al, 1986, Obradovich et al., 1989; Glass et al., 1995; Albin and Wampler, 1996; Horton and Izett,
257 2005; Fernandes et al., 2019), and U/Pb TIMS zircon single crystal analyses (Fig. 7; Kamo et al.,
258 2002). This (U-Th)/He zircon age suggests that Chesapeake Bay is a late Eocene impact event
259 (Koeberl, 2009), and it also overlaps within 2σ errors with the 33.91 ± 0.05 Ma age of the
260 Eocene-Oligocene boundary (Fig. 7; Brown et al., 2009). However, the more precise inverse
261 isochron $^{40}\text{Ar}/^{39}\text{Ar}$ age of 34.86 ± 0.32 Ma (Fernandes et al., 2019), obtained from NA tektites
262 and Chesapeake Bay impact melt lithologies, does not overlap with the Eocene-Oligocene
263 boundary (Fig. 7), which suggests that there is no connection between the Chesapeake impact
264 structure and the Eocene-Oligocene extinction event. This is confirmed by the observation that
265 the NA microtektite layer is located metres below the global stratigraphic Eocene/Oligocene
266 boundary in the Massignano section, Italy (Koeberl, 2009).

267

268 **Conclusions**

269 (U-Th)/He dating of zircon crystals from a distal ejecta sample from ODP drill hole
270 1073A yields a range of dates from 33.49 ± 0.94 to 305.1 ± 8.6 Ma. The two youngest zircon
271 grains, which show evidence of shock metamorphism, yield a weighted mean date of $33.99 \pm$
272 0.71 Ma. This date is consistent with previous geochronological results (Fig. 7), and is
273 interpreted as the shock-induced zircon (U-Th)/He resetting age of the Chesapeake Bay impact

274 event. Our results provide evidence that it is possible to obtain impact crater formation ages via
275 (U-Th)/He dating of carefully characterized distal ejecta samples.

276

277 **Acknowledgements**

278 Primary support for the work done at ASU was provided by the U.S. National Science
279 Foundation (EAR-9048143). Any use of trade, firm, or product names is for descriptive purposes
280 only and does not imply endorsement by the U.S. Government. We would like to thank M.
281 Schmieder and F. Jourdan for their constructive reviews of this manuscript.

282

283 **References**

284 Albin E. F., and Wampler J. M. 1996. New potassium-argon ages for georgiites and the Upper
285 Eocene Dry Branch Formation (Twiggs Clay Member): Inferences about tektite stratigraphic
286 occurrence (abstract). 27th Lunar and Planetary Science Conference, p. 5-6.

287

288 Andrews G. D. M., Schmitt A. K., Busby C. J., Brown S. R., Blum P., and Harvey J. C. 2016.
289 Age and compositional data of zircon from sepiolite drilling mud to identify contamination of
290 ocean drilling samples. *Geochemistry, Geophysics, Geosystems* 10.1002/2016GC006397

291

292 Austin J. A., Christie-Blick N., Malone M.J., and Shipboard Scientific Party. 1998. Proceedings
293 of the Ocean Drilling Program initial reports volume 174A, College Station, Texas.

294

295 Biren M. B., van Soest M. C., Wartho J-A., and Spray J. G. 2014. Dating the cooling of exhumed
296 central uplifts of impact structures by the (U-Th)/He method: A case study at Manicouagan.
297 *Chemical Geology* 377:56-71.

298

299 Biren M. B., van Soest M. C., Wartho J-A., Hodges K. V., and Spray J. G. 2016. Diachroneity of
300 the Clearwater West and Clearwater East impact structures indicated by the (U-Th)/He dating
301 method. *Earth and Planetary Science Letters* 453:56-66.

302

303 Böhlke, J. K., de Laeter, J. R., de Bièvre, P., Hidaka, H., Peiser, H. S., Rosman, K. J. R., and
304 Taylor, P. D. P. 2005. Isotopic compositions of the elements, 2001. *Journal of Physical and*
305 *Chemical Reference Data* 34:57-67.

306

307 Bohor B. F., Betterton W. J., and Krogh T. E. 1993. Impact-shocked zircons: Discovery of
308 shock-induced textures reflecting increasing degrees of shock metamorphism. *Earth and*
309 *Planetary Science Letters* 199:419-424.

310

311 Bottomley R. J. 1982. ^{40}Ar - ^{39}Ar dating of melt rock from impact craters. Ph.D. thesis, University
312 of Toronto, Canada.

313

314 Bottomley R. J., York D., and Grieve R. A. F. 1979. Possible source craters for the North
315 American tektites – a geochronological investigation (abstract). *Transactions of American*
316 *Geophysical Union EOS* 60:309.

317

318 Brown R.E., Koeberl C., Montanari A., and Bice D.M. 2009. Evidence for a change in
319 Milankovitch forcing caused by extraterrestrial events at Massignano, Italy, Eocene-Oligocene
320 Boundary GSSP In *The late Eocene Earth: Hothouse, Icehouse, and Impacts*, edited by Koeberl,
321 C., and Montanari, A. *Geological Society of America Special Paper* 452:119-137.

322

323 Collins G. S., and Wünnemann K. 2005. How big was the Chesapeake Bay impact? Insight from
324 numerical modeling. *Geology* 33:925–928.

325

326 Corfu F., Hanchar J. M., Hoskin P. W. O., and Kinny P. 2003. Atlas of zircon textures. *Reviews*
327 *in Mineralogy and Geochemistry* 51:469-500.

328

329 Deutsch A., and Koeberl C. 2006. Establishing the link between the Chesapeake Bay impact
330 structure and the North American tektite strewn field: The Sr-Nd isotopic evidence. *Meteoritics*
331 *and Planetary Science* 41:689–703.

332

333 Farley K. A., Wolf R., and Silver L. 1996. The effects of long alpha-stopping distances on (U-
334 Th)/He ages. *Geochimica et Cosmochimica Acta* 60:4223-4229.
335

336 Fernandes, V., Hopp, J., Schwarz, W.H., Fritz, J.P., Trieloff, M., Povenmire, H. 2019.
337 ⁴⁰Ar-³⁹Ar step heating ages of North American tektites and of impact melt rock samples from the
338 Chesapeake Bay impact structure. *Geochimica et Cosmochimica Acta* (in press).
339

340 Fleischer R. L., and Price P. B. 1964. Fission track evidence for the simultaneous origin of
341 tektites and other natural glasses. *Geochimica et Cosmochimica Acta* 28:755-760.
342

343 Garlick G. D., Naeser C. W., and O'Neil J. R. 1971. A Cuban tektite. *Geochimica et*
344 *Cosmochimica Acta* 35:731-734.
345

346 Gentner W., Storzer D., and Wagner G.A. 1969. New fission track ages of tektites and related
347 glasses. *Geochimica et Cosmochimica Acta* 33:1075-1081.
348

349 Gibson R. L., Townsend G. N., Horton J. W., and Reimold W. U. 2009. Pre-impact
350 tectonothermal evolution of the crystalline basement-derived rocks in the ICDP-USGS Eyreville-
351 B core, Chesapeake Bay impact structure. In *The ICDP-USGS Deep Drilling Project in the*
352 *Chesapeake Bay impact structure: Results from the Eyreville core holes*, edited by Gohn G. S.,
353 Koeberl C., Miller K. G., and Reimold W. U. Geological Society of America Special Papers
354 458:235-254.
355

356 Glass B. P. 2002. Upper Eocene impact ejecta/spherule layers in marine sediments. *Chemie der*
357 *Erde Geochemistry* 62:173-96.
358

359 Glass, B.P. and Wu, J., 1993. Coesite and shocked quartz discovered in the, Australasian and
360 North American, microtektite layers. *Geology*, 21:435-438.
361

362 Glass B. P., and Liu S. 2001. Discovery of high-pressure ZrSiO₄ polymorph in naturally
363 occurring shock-metamorphosed zircons. *Geology* 29:371-373.

364

365 Glass B. P., Baker R. N., Storzer D., and Wagner G.A. 1973. North American microtektites from
366 the Caribbean Sea and their fission track age. *Earth and Planetary Science Letters* 19:184-192.

367

368 Glass B. P., Hall C. M., and York D. 1986. $^{40}\text{Ar}/^{39}\text{Ar}$ laser-probe dating of North American
369 tektite fragments from Barbados and the age of the Eocene-Oligocene boundary. *Chemical*
370 *Geology: Isotope Geoscience Section* 59:181–86.

371

372 Glass B. P., Koeberl C., Blum J. D., Senftle F., Izett G. A., Evans B. J., Thorpe A. N., Povenmire
373 H., and Strange R. L. 1995. A Muong Nong-type Georgia tektite. *Geochimica et Cosmochimica*
374 *Acta* 59: 4071–82.

375

376 Gohn G. S., Koeberl C., Miller K. G., Reimold W. U., Browning J. V., Cockell C. S., Horton Jr.
377 J. W., and Kenkmann, T. 2008. Deep drilling into the Chesapeake Bay impact structure. *Science*
378 320:1740-1745.

379

380 Harris R. S., Roden M. S., Schroeder P. A., Holland S. M., Duncan M. S., and Albin E. F. 2004.
381 Upper Eocene impact horizon in east-central Georgia. *Geology* 32:717-720.

382

383 Horton, J. W., Jr., and Izett G. A. 2005. Crystalline-rock ejecta and shocked minerals of the
384 Chesapeake Bay impact structure: The USGS-NASA Langley corehole, Hampton, Virginia, with
385 supplement constraints on the age of the impact. In *Studies of the Chesapeake Bay impact*
386 *structure*, edited by Horton Jr. J. W., Powars D. S., and Gohn G. S. U.S. Geological Survey,
387 Reston, Virginia. pp. E1–E29.

388

389 Horton, J. W., Jr., Kunk, M. J., Belkin, H. E., Aleinikoff, J. N., Jackson, J. C., and Chou, I-M.
390 2009. Evolution of crystalline target rocks and impactites in the Chesapeake Bay impact
391 structure, ICDP-USGS Eyreville B core. In *The ICDP-USGS Deep Drilling Project in the*
392 *Chesapeake Bay Impact Structure: Results from the Eyreville Core Holes*, edited by Gohn, G. S.,
393 Koeberl, C., Miller, K. G., and Reimold, W. U. Geological Society of America Special Paper
394 458:277-316.

395
396 Hourigan J. K., Reiners P. W., and Brandon M. T. 2005. U-Th zonation-dependent alpha-
397 ejection in (U-Th)/He chronometry. *Geochimica et Cosmochimica Acta* 69:3349-3365.
398
399 Jourdan F., Reimold W. U., and Deutsch A. 2012. Dating terrestrial impact structures. *Elements*
400 8:49-53.
401
402 Kamo S. L., Reimold W. U., Krogh, T. E., and Colliston W. P. 1996. A 2.023 Ga age for the
403 Vredefort impact event and a first report of shock metamorphosed zircons in pseudotachylitic
404 breccias and granophyre. *Earth and Planetary Science Letters* 144:369-387.
405
406 Kamo S. L., Krogh T. E., Glass B. P., and Liu S. 2002. U-Pb study of shocked zircons from the
407 North American microtektite layer (abstract). 33rd Lunar and Planetary Science Conference,
408 abstract #1643.
409
410 Kenny, G.G., Schmieder, M., Whitehouse, M.J., Nemchin, A.A., Morales, L.F., Buchner, E.,
411 Bellucci, J.J. and Snape, J.F., 2019. A new U-Pb age for shock-recrystallised zircon from the
412 Lappajärvi impact crater, Finland, and implications for the accurate dating of impact events.
413 *Geochimica et Cosmochimica Acta*, 245:479-494.
414
415 Koeberl C. 2009. Late Eocene impact craters and impactoclastic layers – An overview. In *The*
416 *late Eocene Earth: Hothouse, Icehouse, and Impacts*, edited by Koeberl, C., and Montanari, A.
417 *Geological Society of America Special Paper* 452:17-26.
418
419 Koeberl C., Poag C. W., Reimold W. U., and Brandt D. 1996. Impact origin of the Chesapeake
420 Bay structure and the source of the North American tektites. *Science* 271:1263-1266.
421
422 Liu S., and Glass B. P. 2001. Upper Eocene impact ejecta/spherule layers in marine sediments:
423 New sites. 32nd Lunar and Planetary Science Conference, abstract #2027.
424

425 Liu S., Papanastassiou D. A., Ngo H. H., and Glass B. P. 2006. Sr and Nd analyses of upper
426 Eocene spherules and their implications for target rocks. *Meteoritics and Planetary Science*
427 41:705-714.

428

429 Mercer C. M., and Hodges K. V. 2016. ArAR – A software tool to promote the robust
430 comparison of K-Ar and $^{40}\text{Ar}/^{39}\text{Ar}$ dates published using different decay, isotopic, and monitor-
431 age parameters. *Chemical Geology* 440:148-163.

432

433 Obradovich J., Snee L. W., and Izett G. A. 1989. Is there more than one glassy impact layer in
434 the Late Eocene? (abstract). *Geological Society of America Abstracts with Program* 21:134.

435

436 Poag C. W., Powars D. S., Poppe L. J., Mixon R. B., Edwards L. E., Folger D. W., and Bruce S.
437 1992. Deep Sea Drilling Project Site 612 bolide event: New evidence of a late Eocene impact-
438 wave deposit and a possible impact site, US east coast. *Geology* 20:771-774.

439

440 Poag C. W., Powars D. S., Poppe L. J., and Mixon R. B. 1994. Meteoroid mayhem in Ole
441 Virginny: Source of the North American tektite strewn field. *Geology* 22:691-694.

442

443 Reiners, P.W., Spell, T.L., Nicolescu, S. and Zanetti, K.A., 2004. Zircon (U-Th)/He
444 thermochronometry: He diffusion and comparisons with $^{40}\text{Ar}/^{39}\text{Ar}$ dating. *Geochimica et*
445 *Cosmochimica Acta* 68:1857-1887.

446

447 Renne, P.R., Balco, G., Ludwig, K.R., Mundil, R. and Min, K. 2011. Response to the comment
448 by WH Schwarz et al. on “Joint determination of ^{40}K decay constants and $^{40}\text{Ar}^*/^{40}\text{K}$ for the Fish
449 Canyon sanidine standard, and improved accuracy for $^{40}\text{Ar}/^{39}\text{Ar}$ geochronology” by PR Renne et
450 al.(2010). *Geochimica et Cosmochimica Acta* 75:5097-5100.

451

452 Reynolds J. H. 1960. Rare gases in tektites. *Geochimica et Cosmochimica Acta* 20:101-114.

453

454 Simonson B. M., and Glass B. P. 2004. Spherule layers – records of ancient impacts. *Annual*
455 *Review of Earth and Planetary Sciences* 32:329-361.

456
457
458
459
460
461
462
463
464
465
466
467
468
469
470
471
472
473
474
475
476
477
478
479
480
481
482
483
484

Schmieder, M. and Jourdan, F., 2013. The Lappajärvi impact structure (Finland): Age, duration of crater cooling, and implications for early life. *Geochimica et Cosmochimica Acta* 112:321-339.

Schmieder, M., Tohver, E., Jourdan, F., Denyszyn, S.W. and Haines, P.W. 2015. Zircons from the Acraman impact melt rock (South Australia): Shock metamorphism, U–Pb and $^{40}\text{Ar}/^{39}\text{Ar}$ systematics, and implications for the isotopic dating of impact events. *Geochimica et Cosmochimica Acta* 161:71-100.

Schmieder, M., Kennedy, T., Jourdan, F., Buchner, E. and Reimold, W.U., 2018. A high-precision $^{40}\text{Ar}/^{39}\text{Ar}$ age for the Nördlinger Ries impact crater, Germany, and implications for the accurate dating of terrestrial impact events. *Geochimica et Cosmochimica Acta* 220:146-157.

Storzer D., and Wagner G. A. 1971. Fission track ages of North American tektites. *Earth and Planetary Science Letters* 10:435-440.

Storzer D., and Wagner G. A. 1977. Fission track dating of meteorite impacts. *Meteoritics* 12:368-369.

Timms, N.E., Erickson, T.M., Pearce, M.A., Cavosie, A.J., Schmieder, M., Tohver, E., Reddy, S.M., Zanetti, M.R., Nemchin, A.A. and Wittmann, A. 2017. A pressure-temperature phase diagram for zircon at extreme conditions. *Earth-Science Reviews*, 165:185-202.

Ukstins Peate I., van Soest M. C., Wartho J-A., Cabrol, N. A., Grin E., Piatek J., and Chong G. 2010. A novel application of (U-Th)/He geochronology to constrain the age of small, young meteorite impact craters: A case study of the Monturaqui crater, Chile (abstract). 41st Lunar and Planetary Science Conference, abstract #2161.

485 van Soest M. C., Hodges K. V., Wartho J-A., Biren M. B., Monteleone B. D., Ramezani J.,
486 Spray J. G., and Thompson L. M. 2011. (U-Th)/He dating of terrestrial impact structures: The
487 Manicouagan example. *Geochemistry, Geophysics, Geosystems* 10.1029/2010GC003465
488

489 Wartho J-A., van Soest M. C., King Jr. D. T., and Petruny L. W. 2012. An (U-Th)/He age for the
490 shallow-marine Wetumpka impact structure, Alabama, USA. *Meteoritics and Planetary Science*
491 47:1243-1255.

492

493 Wielicki M. M., Harrison T. M., and Stockli D. 2014. Dating terrestrial impact structures: U-Pb
494 depth profiles and (U-Th)/He ages of zircon. *Geophysical Research Letters* 41:4168-4175.
495

496 Wittmann A., Kenkmann T., Schmitt R. T., and Stöffler D. 2006. Shock-metamorphosed zircon
497 in terrestrial impact craters. *Meteoritics and Planetary Science* 41:433-454.
498

499 Wittmann A., Reimold W. U., Schmitt R. T., Hecht L., and Kenkmann T. 2009a. The record of
500 ground zero in the Chesapeake Bay impact crater – suevites and related rocks. In *The ICDP-*
501 *USGS Deep Drilling Project in the Chesapeake Bay impact structure: Results from the Eyreville*
502 *core holes*, edited by Gohn G. S., Koeberl C., Miller K. G., and Reimold W. U. Geological
503 Society of America Special Paper 458:349-376.
504

505 Wittmann A., Schmitt R. T., Hecht L., Kring D. A., Reimold W. U., and Povenmire H. 2009b.
506 Petrology of impact melt rocks from the Chesapeake Bay crater, USA. In *The ICDP-USGS Deep*
507 *Drilling Project in the Chesapeake Bay impact structure: Results from the Eyreville core holes*,
508 edited by Gohn G. S., Koeberl C., Miller K. G., and Reimold W. U. Geological Society of
509 America Special Paper 458:377-396.
510

511 Young K. E., van Soest M. C., Hodges K. V., and Watson E.B. 2013a. Impact thermochronology
512 and the age of the Haughton impact structure, Canada. *Geophysical Research Letters* 40:3836-
513 3840.
514

515 Young K. E., Hodges, K. V., van Soest M. C., Wartho J-A., Mercer C. M., Osinski G. R., and
516 Marion C. L. 2013b. Geochronology and thermochronology of the Mistastin Lake impact
517 structure, Labrador, Canada (abstract). 2013 American Geophysical Union Fall Conference,
518 abstract #P34C-02.
519
520 Zähringer J. 1963. K-Ar measurements of tektites. Radioactive Dating, Proceedings of the
521 symposium on radioactive dating held by the International Atomic Energy Agency in co-
522 operation with the Joint Commission on Applied Radioactivity in Athens, 19-23 November
523 1962. International Atomic Energy Agency, Vienna p. 289-299.

Author Manuscript

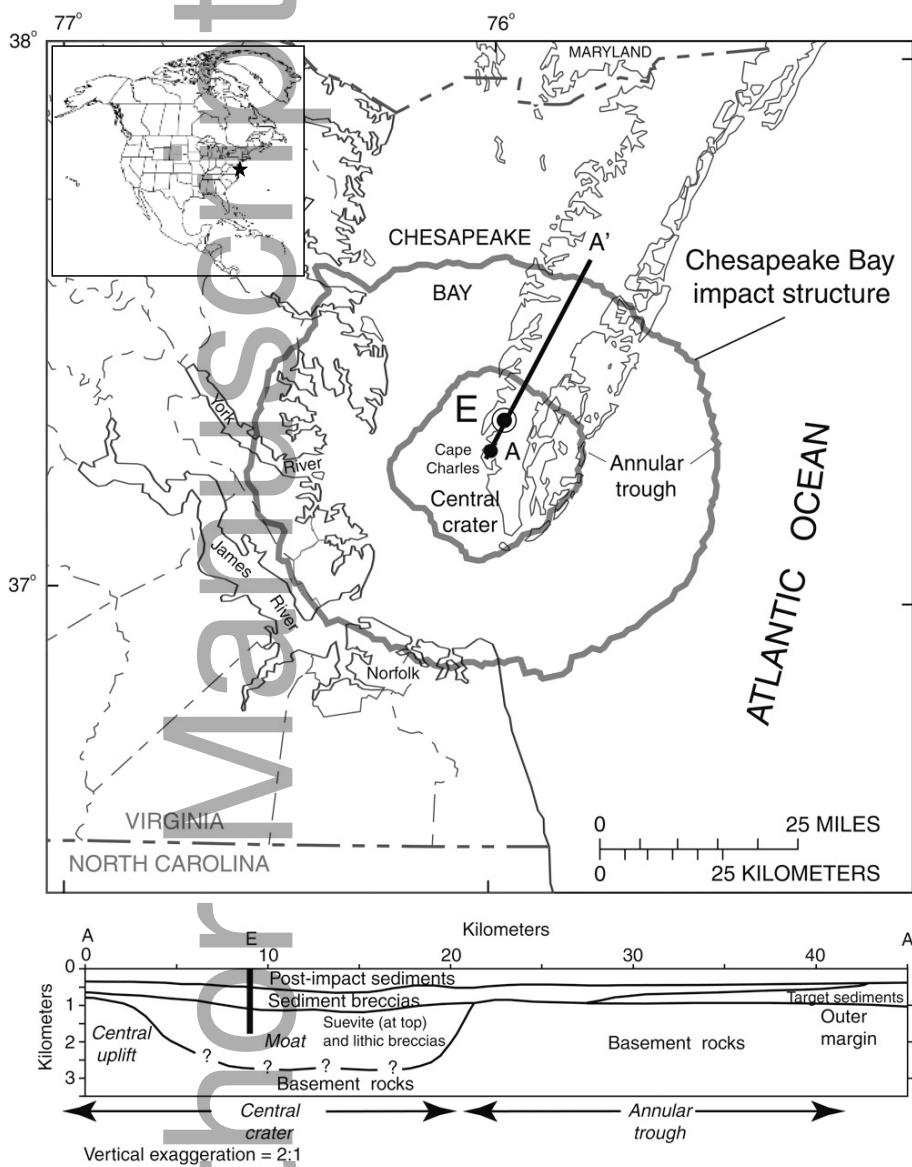


Fig. 1. Map and generalized cross-section (A-A') of the Chesapeake Bay impact structure, showing the location of the Eyreville drill site (E; map modified from Gohn et al., 2008). Inset map shows the location (black star) of the Chesapeake Bay impact crater in North America.

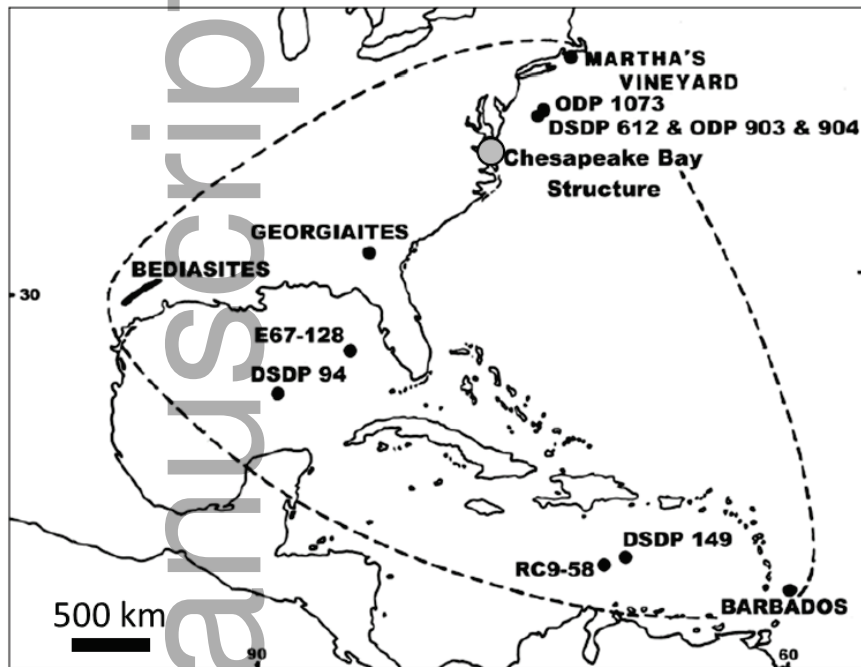


Fig. 2. Map of the North American tektite strewn field (modified map from Glass, 2002), showing onshore tektite locations in Texas (bediasites), Georgia (georgiaites), Massachusetts (Martha's Vineyard), and Barbados. Offshore tektite and microtektite locations include the Caribbean Sea (DSDP 149 and Core RC9-58), Gulf of Mexico (DSDP 94 and Core E67-128), and continental shelf in the north-west Atlantic Ocean (DSDP 612 and ODP site 904). Unmelted ejecta has been found at all the offshore core sites except for Core E67-128 (Glass and Wu, 1993; Glass and Liu 2001). The (U-Th)/He dated zircons in this study were sampled from ODP site 1073 hole A.

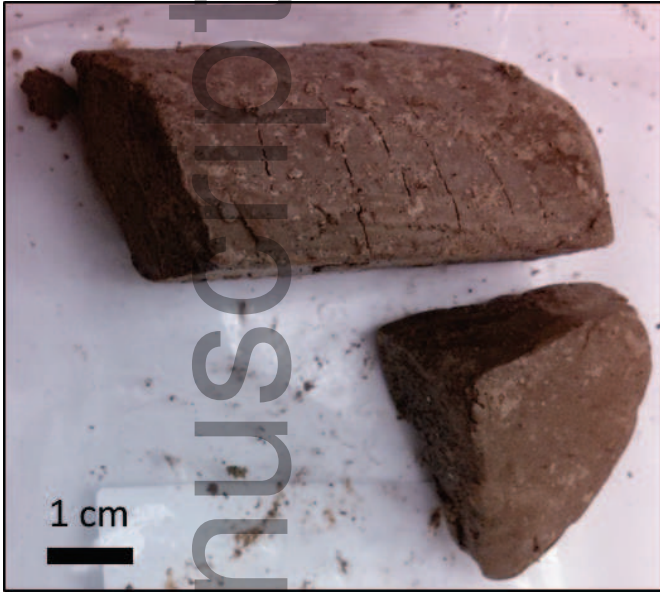


Fig. 3. ~30 cm³ unconsolidated glauconite-bearing late Eocene sediment obtained from ODP site 1073, hole A, core 72, section 4, interval 83-94 cm.

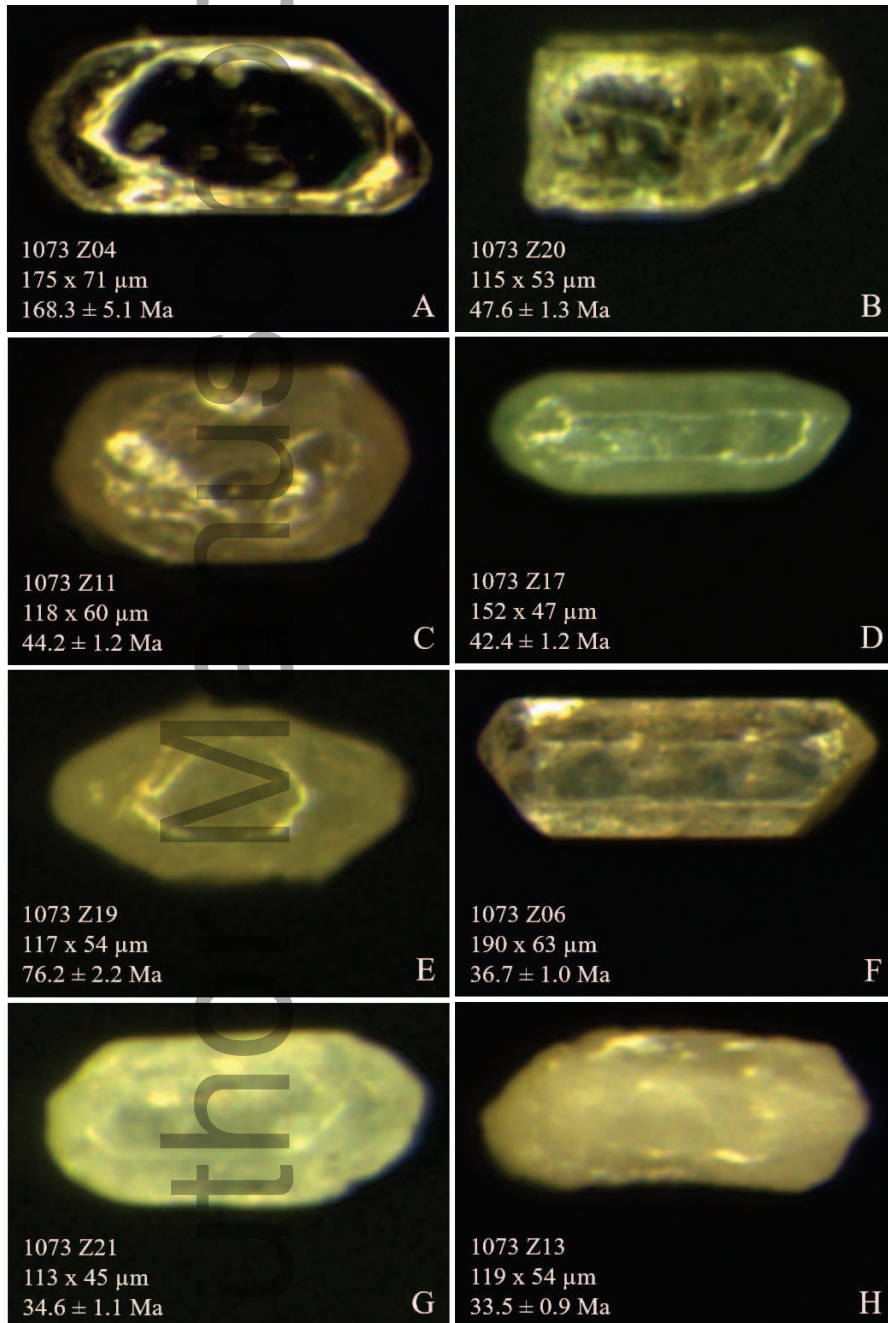


Fig. 4. Binocular light microscope photomicrographs of the eight youngest zircon crystals dated using the (U-Th)/He technique, showing the (U-Th)/He ages (2σ uncertainties), and lengths and average widths of the crystals: (A) 1073 Z04 – a clear euhedral zircon crystal. (B) 1073 Z20 – a transparent subhedral zircon that is missing one crystal termination. (C) 1073 Z11 – a subhedral, slightly rounded, semi-translucent zircon crystal. (D) 1073 Z17 – a light-colored translucent zircon. (E) 1073 Z19 – a semi-translucent subhedral zircon. (F) 1073 Z06 – a translucent euhedral zircon. (G) 1073 Z21 – a white-colored translucent zircon crystal that has the appearance of an uncooked grain of rice. (H) 1073 Z13 – a white semi-opaque zircon crystal that has the appearance of a cooked grain of rice.

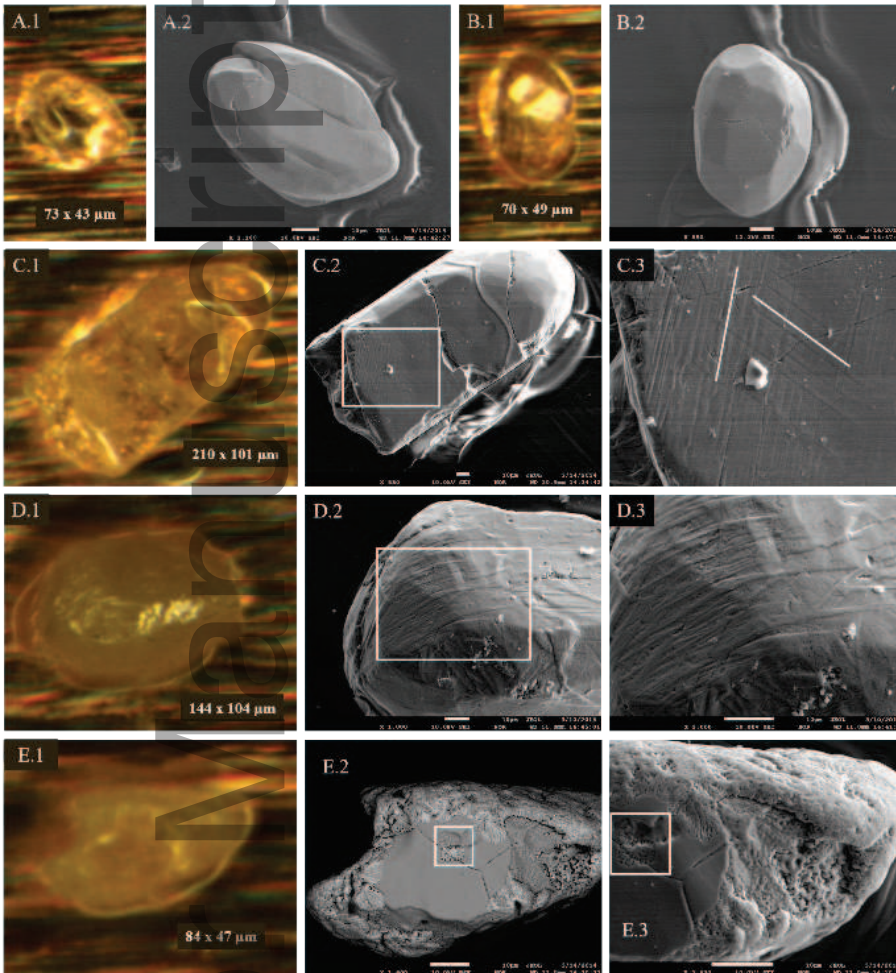


Fig. 5. Binocular light microscope photomicrographs and secondary electron (SE) and back-scattered electron (BSE) images of undated zircon grains and grain fragments from Late-Eocene unconsolidated sediment from ODP Site 1073, hole A. Light microscope (A.1 and B.1) and SE images (A.2 and B.2) of two unshocked zircons. Light microscope (C.1 and D.1) and SE images (C.2-C.3 and D.2-D.3) of two zircon grains with multiple linear/planar features, interpreted to be planar deformation features. The white boxes in 5C.2 and 5D.2 show the magnified areas in 5C.3 and 5D.3, respectively. The white lines in Fig. 5C.3 highlight the two sets of planar deformation features. Light microscope (5E.1) and BSE (5E.2) and SE (5E.3) images of a zircon grain that shows a granular texture, and dendritic textures caused by partial decomposition of zircon to baddeleyite and silica (confirmed by EDS analyses on these phases). For ease of comparison, the white boxes in the BSE (5E.2) and SE (5E.3) photomicrographs indicate the same region in this zircon grain. The white scale bars in the SE and BSE photomicrographs are all 10 μm . The horizontal streaks in the SE images 5B.2, 5C.2 and 5C.3) were caused by sample surface charging effects.

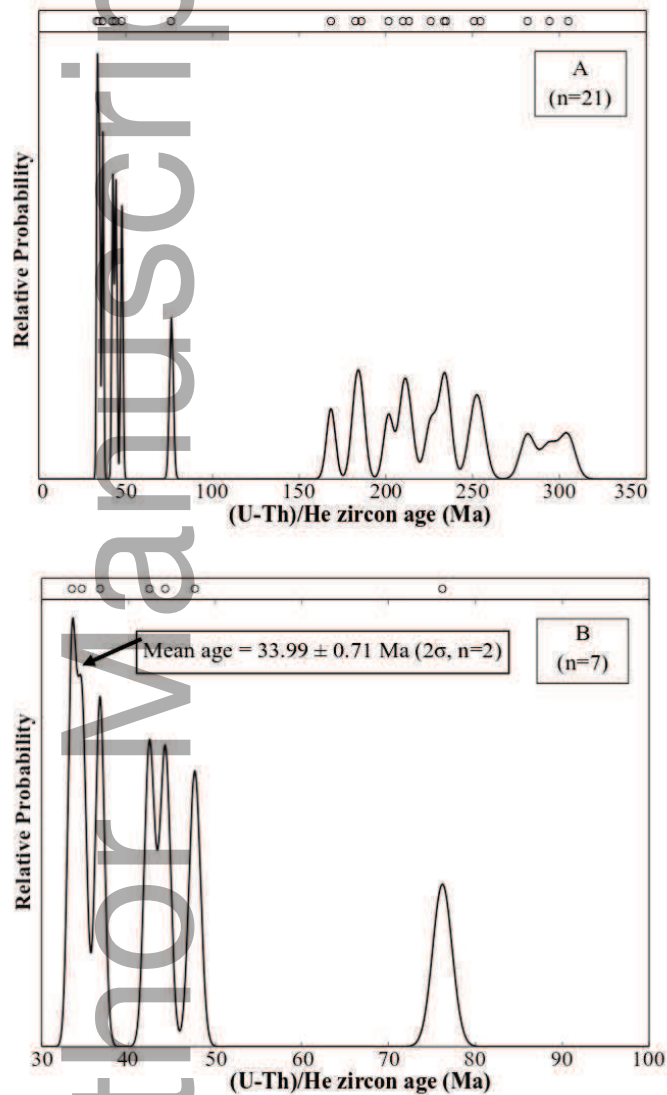


Fig. 6. Probability density plots of (U-Th)/He zircon ages ranging from (A) 33.49 ± 0.94 to 305.1 ± 8.6 Ma (2σ) for all 21 zircon grains, and (B) the 7 youngest zircon grain ages. The individual (U-Th)/He ages are shown as white circles in the upper portions of the plots.

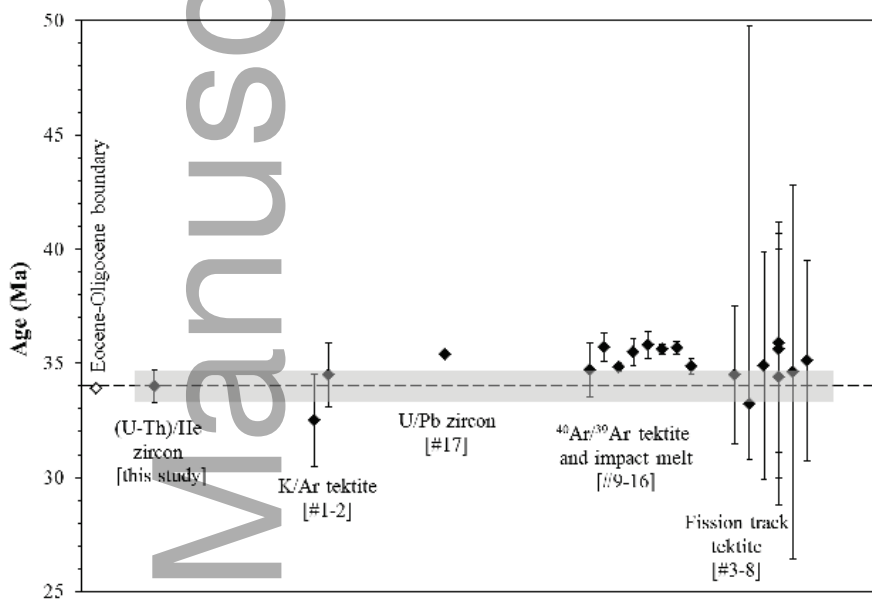


Fig. 7. Plot of previous geochronological ages (fission track, K/Ar, $^{40}\text{Ar}/^{39}\text{Ar}$, and U/Pb; black diamonds) compared with our new (U-Th)/He age for the Chesapeake Bay and NAT strewn field (2σ uncertainties). The numbers (#) refer to references quoted in Table 1. The dashed line and grey box indicate our 33.99 ± 0.71 Ma inverse-variance weighted mean (U-Th)/He age and 2σ uncertainty envelope, respectively. The white diamond shows the Eocene-Oligocene boundary age of 33.91 ± 0.05 Ma (Brown et al., 2009; 2σ errors are smaller than the symbol size).

Deleted: ¶

Page Break

<object>¶

Table 1. Previous geochronological ages for the Chesapeake Bay impact structure and associated NAT deposits. ¶

Formatted: English (United Kingdom)